



Influence of Superheated Steam Temperature and Moisture Exchange on the Inactivation of *Geobacillus stearothermophilus* Spores in Wheat Flour-Coated Surfaces

Hyeon Woo Park¹ · V. M. Balasubramaniam^{1,2} · Abigail B. Snyder³ · J. A. Sekhar⁴

Received: 1 March 2022 / Accepted: 17 May 2022

© The Author(s), under exclusive licence to Springer Science+Business Media, LLC, part of Springer Nature 2022

Abstract

Sanitation in dry food processing environments is a major challenge for the industry. The influence of superheated steam (SH) temperatures (125 to 250 °C) on the inactivation of spores on selected coupon surfaces (stainless steel, rubber, and concrete) coated with wheat flour as a model food soil residue was investigated using a bench scale superheating apparatus. Wheat flour inoculated with *Geobacillus stearothermophilus* (7.62 ± 0.12 log CFU/g) coated on the coupon surfaces served as the model food residue. Among the surfaces tested, temperature of concrete increased faster [time constant (τ) < 89.0 s] than that of stainless steel (τ < 173.6 s). As a consequence, wheat flour coated on concrete dehydrated faster [moisture diffusivity (D_m) > 1.17×10^{-4} mm²/s] than those on the stainless steel (D_m > 0.76×10^{-4} mm²/s). Hence, *Geobacillus stearothermophilus* spores suspended on stainless steel were inactivated faster than that of concrete and rubber (p < 0.05). The time required for a 5-log reduction at 250 °C were 180 s and 240 s, on stainless steel and concrete surfaces, respectively. A mathematical model that considered surface temperature, food residue moisture content, and SH inversion temperature adequately described spore inactivation during SH treatment.

Keywords Dry surface sanitation · Spore inactivation · Inactivation kinetics · Inversion temperature · Heat and mass transfer · Mathematical modeling

Abbreviations

B_f	Bias factor
D_m	Moisture diffusivity (mm ² /s)
D_{ref}	D Value at a reference condition (s)
L	Thickness (mm)
M	Moisture content (% d.b.)
M_{cond}	Moisture content after initial condensation (% d.b.)
M_{eq}	Equilibrium moisture content (% d.b.)
M_i	Initial moisture content (% d.b.)

MR	Moisture ratio
M_{ref}	Reference moisture content (% d.b.)
N	Surviving microbial count (CFU/g)
N_0	Initial microbial count (CFU/g)
N_m	Estimated microbial count (CFU/g)
n	Number of data points
p	Number of parameters
RH	Relative humidity of superheated steam (%)
RH_{ref}	Reference relative humidity (%)
RSME	Root mean square error
T	Temperature (°C)
t	Total treatment time (s)
t_{cond}	Condensation time (s)
T_{iv}	Inversion temperature (°C)
T_{ref}	Reference temperature (°C)
T_{SH}	Superheated steam temperature (°C)
z_T	Temperature sensitivity of <i>Geobacillus stearothermophilus</i> spore (°C)
z_M	Moisture content sensitivity of <i>G. stearothermophilus</i> spore (% d.b.)
z_{RH}	Relative humidity sensitivity of <i>G. stearothermophilus</i> spore (%)

✉ V. M. Balasubramaniam
balasubramaniam.1@osu.edu

¹ Department of Food Science and Technology, The Ohio State University, Columbus, OH 43210, USA

² Department of Food Agricultural and Biological Engineering, The Ohio State University, Columbus, OH 43210, USA

³ Department of Food Science, Cornell University, Ithaca, NY 14853, USA

⁴ MHI Inc., Cincinnati, OH 45215, USA

α	A constant for initial condensation during superheated steam treatment
β	A constant for drying during superheated steam treatment
τ	Time constant (s)
<i>D value</i>	Decimal reduction time (s)

Introduction

Prevention of environmental cross-contamination is of paramount importance in ensuring food safety and preventing spoilage, particularly in dry environments. In dry food processing facilities, the traditional wet sanitation approaches are not recommended because moisture may cause the growth of foodborne pathogens in otherwise dry environments, putrefaction of food products, and the quality change of food products if they are hygroscopic in nature (Beuchat et al., 2013; Burnett & Hagberg, 2014; Moerman & Mager, 2016). Thus, as a general rule, dry sanitation is preferred in dry food processing facilities.

Superheated steam is steam that has been superheated above its saturation temperature at a given pressure (Van Deventer & Heijmans, 2001). Application of superheated steam as a food dehydration technology has been well investigated, but limited studies evaluated it as a potential dry sanitation method (Park et al., 2021). Superheated steam (generally 125 to 300 °C) treatment reportedly inactivates vegetative bacteria and spores on dry surfaces rapidly (Ban et al., 2014; Jo et al., 2019; Kim et al., 2020; Park et al., 2021). Since it uses only water and heat, it can be considered environmentally friendly sanitation method to decontaminate dry food plant surfaces. Various factors reportedly affect the sanitation efficacy of superheated steam, such as temperature and moisture of the food soil residue and the relative humidity of superheated steam (Kondjoyan & Portanguen, 2008; Park et al., 2021).

Food processing plants employ diverse materials including stainless steel, black metals, tin, concrete, and rubber. The role of such surfaces as a vehicle for transmission of microbial contaminants has been recognized (Marriott et al., 2016). Attention also must be paid on how different surface properties influence microbial sanitation efficacy, for example, the thermophysical properties and porosity, which may affect heat transfer as well as microbiological inactivation during superheated steam treatment.

Within the drying literature, the “inversion temperature” concept is used to differentiate superheated steam drying from hot air drying (Volchkov et al., 2007). Inversion temperature is the temperature at which dehydration rate from superheated steam and hot air is equal (Schwartz & Brocker, 2002). The drying rates by superheated steam are faster than those by hot air drying at temperatures above the inversion temperature. Under such conditions, contrary

to wet steam, the relative humidity decreases rapidly with increasing superheated steam temperature. For example, the relative humidity of superheated steam at 150 °C and 250 °C are 21.3% and 2.6. Above the inversion temperature, superheated steam drying is faster than hot air drying because of the higher heat transfer coefficients of superheated steam.

The inversion temperatures of superheated steam during drying of various foods have been reported. This includes shrimp (140–150 °C), sugar beet pulp (130 °C), paddy rice (170 °C), potato (145–165 °C), and banana (160 °C) (Hamawand et al., 2014; Prachayawarakorn et al., 2002; Pronyk et al., 2004; Swasdisevi et al., 2013; Tang & Cenkowski, 2000). However, limited studies reported the role of inversion temperature in spore inactivation during superheated steam treatment.

It is difficult to sanitize microbial contaminants in food soil residues using conventional dry sanitation methods. Wheat flour, a common low-moisture content food material, was chosen as model food soil residue to investigate the superheated steam efficacy on microbial inactivation in food residue. Our study employed *Geobacillus stearothermophilus*, commonly used as surrogate organism for thermal sterilization processes as test organism for the study.

The objectives of this study were to (1) investigate the influence of superheated steam temperatures and moisture exchange between food residue (adhered to different dry surfaces) and superheated steam environment on the inactivation of *G. stearothermophilus* spores and (2) to develop a mathematical model to estimate the inactivation of *G. stearothermophilus* spore during superheated steam treatment.

Materials and Methods

Preparation of Spore Crop

G. stearothermophilus ATCC 7953 was purchased from the American Type Culture Collection (Manassas, VA, USA). *G. stearothermophilus* was grown in nutrient broth (Difco, Detroit, MI, USA) for 24 h at 55 °C. After the second cultivation in nutrient broth, 500 µl of the culture was spread plated on nutrient agar (Difco, Detroit, MI, USA) containing 10 ppm MnSO₄ (Fisher Scientific, Pittsburgh, PA, USA) to induce sporulation. After 10 days of incubation at 55 °C, more than 90% sporulation was observed by microscopic examination. The bacterial spores were harvested by flooding with 10 ml sterile distilled water. The spore suspension was washed five times at 8,000 g for 20 min at 4 °C, sonicated for 10 min at 38.5 kHz and 270 W (Crest Ultrasonic, ETL Testing Laboratories, Inc., Cortland, NY, USA), and heated at 80 °C for 10 min to destroy any remaining

vegetative cells. The collected spore pellet was stored at 4 °C until needed.

Sample Preparation and Inoculation

The study used coupons made from stainless steel (AISI 316, American Iron and Steel Institute, Washington, DC., USA), rubber (acrylonitrile-butadiene rubber, McMaster-Carr, Elmhurst, IL, USA), and concrete (Anchoring cement, Quikrete, Atlanta, GA, USA) because these are common surface materials in food processing environments (Cai et al., 2020; Marriott et al., 2016). The thermal conductivity, specific heat, and density of these coupon materials at 125 °C were reported to be 15.5 W/(m·K), 523.1 J/(kg·K), and 7910.5 kg/m³ for stainless steel; 1.5 W/(m·K), 925.0 J/(kg·K), and 2295.2 kg/m³ for concrete; and 0.3 W/(m·K), 1960.0 J/(kg·K), and 1178.9 kg/m³ for rubber, respectively (Kim, 1975; Pinedo et al., 2018; Zehfuß et al., 2020). The porosity of concrete was 34.5%, while stainless steel and rubber are non-porous materials (Wang et al., 2018).

Whey flour solution was prepared by thoroughly mixing 4 g of wheat flour (King Arthur Flour, Norwich, VT, USA) with 14 ml of sterile distilled water and 2 ml of the *G. stearothermophilus* spore suspension. Then the solution was applied as thin film using a 3D printed plastic mold over different coupons (34.9 mm × 23.8 mm × 4.8 mm, length × width × thickness) made from different materials (stainless steel, rubber, and concrete). The coupons with flour film (30.9 mm × 19.8 mm × 0.30 mm, length × width × thickness) were subsequently dried in a biosafety hood for 3 h and were transferred to a chamber containing saturated NaNO₂ solution. Coupons were equilibrated for 2 days to obtain a a_w of 0.66 ± 0.01 and a moisture content of 15.5% (d.b.). The population of *G. stearothermophilus* spores in dried flour film on coupons was 7.62 ± 0.12 log CFU/g (i.e., the initial population prior to superheated steam treatment).

Superheated Steam Treatment

Superheated steam experiments were conducted at atmospheric pressure by adapting previously published procedures (Park et al., 2021). Prior to experiments, the treatment chamber was preheated for 1 h to reach a steady-state condition at desired target temperature (125 °C, 150 °C, 170 °C, 210 °C, and 250 °C) using a bench scale 1-kW superheated steam generator (HGA-S, MHI Inc., Cincinnati, OH, USA). The prepared coupon (initially at 25 °C) was mounted on a custom coupon holder and introduced into preheated superheated steam chamber at 2-cm distance from the steam source. After treating coupons for the specific time

interval, coupons were rapidly withdrawn and immediately transferred to a conical tube containing 10 ml of 0.1% peptone water and approximately 5 g of 0.5 mm glass beads. The tubes were suspended in an ice-water bath to stop the thermal process.

During superheated steam treatment, the surface temperature and the moisture content of flour film coating on the surface were monitored to evaluate their influence spore inactivation. A k-type surface thermocouple (Omega Engineering, Norwalk, CT, USA) was attached to the surface of the flour film at its geometric center and continuously recorded the temperature in 1-s interval.

For estimating moisture content of the flour films, samples were withdrawn at specific time intervals. The moisture content of the flour film was measured gravimetrically according to the AOAC method (1990). The moisture content of flour film was reported on a dry basis.

Enumeration of Survivors

Each flour film sample in 10 ml of 0.1% peptone water was homogenized with approximately 5 g of 0.5 mm glass beads for 3 min by using a vortex mixer (Mini Vortexer, Thermo Fisher Scientific, Waltham, MA, USA), and then 100 µl aliquot samples were spread plated on nutrient agar plates directly or after serial dilutions. The plates were incubated for 48 h at 55 °C for enumeration of colonies. To extend the detection limit (100 CFU/g), 1 ml of the homogenized sample was spread-plated onto 3 nutrient agar plates, and the colonies from the 3 plates were summed.

Heat Transfer During Superheated Steam Treatment

During the initial stages of superheated steam treatment, the temperature of the surface changes from the initial value to the boiling point of water (100 °C) as the heat is transferred from superheated steam to the material surface (Ramachandran et al., 2017). Subsequently the surface temperature begins to increase rapidly. Newton's law of heating has been used to describe the temperature profile of food products during heating or cooling processes (Bergman et al., 2011; Carslaw & Jaeger, 1959). Therefore, surface temperature of the flour film during superheated steam treatment can be described by the following relationship:

$$T = T_{SH} + (100 \text{ °C} - T_{SH})e^{-\frac{(t-t_{cond})}{\tau}}, \text{ when } t \geq t_{cond} \quad (1)$$

where T is the surface temperature of flour film (°C), T_{SH} is the superheated steam temperature, τ is time constant (s), t is the processing time (s), and t_{cond} is the time required to reach the saturation temperature (s).

Moisture Exchange During Superheated Steam Treatment

The moisture diffusivity (D_m) provides useful information to understand the moisture movement within the flour film during the superheated steam process. The D_m at any given condition can be estimated using the “methods of slope” technique from the analytical solution of Fick’s second law equation (Marinos-Kouris & Maroulis, 2020). The shape of the flour film was assumed as an infinite slab as the thickness of the flour film (0.30 mm) was much less than its width (19.8 mm). When the sample is assumed to be one-dimensional and to have uniform moisture diffusivity, the D_m of flour film after initial condensation can be defined by Fick’s second law and the analytical solution of Fick’s second law of diffusion as follows:

$$\frac{\partial M}{\partial t} = D_m \frac{\partial^2 M}{\partial x^2} \quad (2)$$

The analytical solution of Fick’s second law of diffusion for an infinite slab,

$$MR = \frac{M - M_{eq}}{M_{cond} - M_{eq}} = \frac{8}{\pi^2} \exp\left(-\frac{\pi^2 D_m (t - t_{cond})}{L^2}\right) \quad (3)$$

where M is the moisture content of flour film (% d.b.), M_{eq} is the equilibrium moisture content of flour (% d.b.), MR is the moisture ratio, and L is the thickness of flour film (mm).

To describe the moisture change of the flour film during superheated steam treatment, the modified Page’s equation was used with the assumption that the moisture content of flour film linearly increases during the initial condensation as follows (Overhults et al., 1973):

$$M(t) = M_i + \alpha \times t, \text{ when } t < t_{cond} \quad (4)$$

$$M(t) = (M_{cond} - M_{eq})e^{-\beta(t-t_{cond})^n} + M_{eq}, \text{ when } t \geq t_{cond} \quad (5)$$

where M_i is the initial moisture content of flour film, α is a constant for initial condensation, and β and n are constants for dehydration.

Modeling Spore Inactivation

To model spore inactivation during superheated steam, we considered both heat and moisture transfer during superheated steam treatment by using models describing temperature and moisture histories during superheated steam treatment (Eqs. (1), (4), and (5)). Model parameters were estimated from the superheated experiments conducted at 125 °C, 170 °C, and 250 °C. Subsequently, these models

were used to estimate the decimal reduction time (D value) of *G. stearothersophilus* spore inactivation. Three different secondary models were evaluated for estimating the inactivation of *G. stearothersophilus* spores on different surfaces (Eqs. (6)–(11)).

These models considered the influence of moisture content, surface temperature, relative humidity, and inversion temperature. For the model fittings, each secondary model was integrated into the log-linear primary model. The study did not consider Weibull model as we have limited prior knowledge of the impact of multiple variables on degree of shouldering or tailing that a particular variable might induce in primary inactivation curves (Casulli et al., 2021).

Model A—considered the contributions of surface temperature and product moisture content Model A is a traditional log-linear temperature model that incorporated log-linear moisture content effects (Eq. (6)).

$$D_{T,M}(t) = D_{ref} \times 10^{\frac{T_{ref}-T(t)}{z_T} + \frac{M_{ref}-M(t)}{z_M}} \quad (6)$$

The integrated form of model A is:

$$\log \frac{N}{N_0} = \int_0^t \frac{-1}{D_{ref} \times 10^{\frac{T_{ref}-T(t)}{z_T} + \frac{M_{ref}-M(t)}{z_M}}} dt \quad (7)$$

where D_{ref} is the D value at the reference conditions (s), T_{ref} is the reference temperature (°C), $T(t)$ is the surface temperature of flour film at total treatment time (t), z_T is the temperature sensitivity of *G. stearothersophilus* spore (°C), M_{ref} is the reference moisture content (% d.b.), $M(t)$ is the moisture content at t (% d.b.), and z_M is the moisture content sensitivity of *G. stearothersophilus* spore (% d.b.). It is worth to note that total treatment time include both come-up time and time the surface is held at the target temperature. N_0 and N are the initial microbial count and the surviving microbial count at t (CFU/g), respectively.

Model B—considered contributions from surface temperature, product moisture content, and relative humidity of the superheated steam In model B, an additional term was incorporated within model A that considered the relative humidity of superheated steam. The relative humidity of superheated steam was not varied over time in this model but was determined based on the temperature of superheated steam (Björk & Rasmuson, 1995). Equation (6) will be modified as follows after incorporating relative humidity term.

$$D_{T,M,RH}(t) = D_{ref} \times 10^{\frac{T_{ref}-T(t)}{z_T} + \frac{M_{ref}-M(t)}{z_M} + \frac{RH_{ref}-RH}{z_{RH}}} \quad (8)$$

The integrated form of model B is:

$$\log \frac{N}{N_0} = \int_0^t \frac{-1}{D_{ref} \times 10^{\frac{T_{ref}-T(t)}{z_T} + \frac{M_{ref}-M(t)}{z_M} + \frac{RH_{ref}-RH}{z_{RH}}}} dt \quad (9)$$

where RH_{ref} is the reference relative humidity (%), RH is the relative humidity of superheated steam at the temperature of superheated steam (%), and z_{RH} is the RH sensitivity of *G. stearothermophilus* spores (%). The RH of superheated steam is defined as the ratio of the partial vapor pressure of superheated steam (i.e., the ambient pressure) to the pressure of saturation steam at the temperature of superheated steam (Tang & Cenkowski, 2001).

Model C—considered contributions from surface temperature, product moisture content, and surface inversion temperature Model C was proposed to incorporate the concept of inversion temperature to describe the temperature sensitivity of *G. stearothermophilus* spores in flour film during superheated steam treatment. In this model, the z_T of *G. stearothermophilus* spores changes at the inversion temperature. Thus, there are two different z_T values in model C for temperatures below and above the inversion temperature as follows:

$$D_{T, M, T_{iv}}(t) = D_{ref} \times 10^{\frac{T_{ref}-T(t)}{z_T} + \frac{M_{ref}-M(t)}{z_M}}, \quad (10)$$

where $z_T = z_{T1}$ when $T < T_{iv}$
and $z_T = z_{T2}$ when $T \geq T_{iv}$

The integrated form of model C is:

$$\log \frac{N}{N_0} = \int_0^t \frac{-1}{D_{ref} \times 10^{\frac{T_{ref}-T(t)}{z_T} + \frac{M_{ref}-M(t)}{z_M}}} dt, \quad (11)$$

where $z_T = z_{T1}$ when $T < T_{iv}$ and $z_T = z_{T2}$ when $T \geq T_{iv}$

where T_{iv} is the inversion temperature (°C).

T_{iv} was determined first at 170 °C and 0% moisture content (d.b.), based on review of prior drying literature of food material (Hamawand et al., 2014; Prachayawarakorn et al., 2002; Pronyk et al., 2004; Swasdisevi et al., 2013; Tang & Cenkowski, 2000) (see the “Role of Inversion Temperature in Spore Inactivation” section for more discussion on inversion temperature and its relationship to microbial inactivation). After determination of T_{iv} , the temperature, M_{eq} , and RH at T_{iv} were used for T_{ref} , M_{ref} , and RH_{ref} , respectively. To derive the parameters for each model, a nonlinear regression analysis was conducted using a nonlinear least squares regression algorithm (*nlinfit*) (Matlab R2013b, The MathWorks, Natick, MA, USA).

Model Validation

To validate the various inactivation models developed, an additional independent set of experiments were conducted

at 150 °C and 210 °C. The root mean square error (RMSE) and the bias factor (B_f) were used to evaluate the model performance (Baranyi et al., 1999). The bias factor indicates by how much on average a model underpredicts ($B_f < 1$) or overpredicts ($B_f > 1$) the spore inactivation. RMSE and B_f were calculated as follows:

$$RMSE = \sqrt{\frac{1}{n-p} \cdot \sum_{i=1}^n [\log(N/N_m)]^2} \quad (12)$$

$$B_f = 10^{\sum_{i=1}^n \log(N/N_m)/n} \quad (13)$$

where n is the number of data points, p is the number of parameters for each model, and N_p is the estimated microbial count from model (CFU/g).

Statistical Analysis

The survival data is based on 6 data points (3 independent superheated steam experiments carried out on different days × 2 enumeration plates for each sample). The moisture content and temperature of samples were measured in triplicate. Multi-way ANOVA and Tukey’s multiple comparison tests at the significance level of 0.05 were performed to evaluate the influence of superheated steam treatment parameters including temperature, treatment time, and type of coupon on the inactivation of *G. stearothermophilus* spores by using SPSS software (SPSS Inc., Chicago, IL, USA).

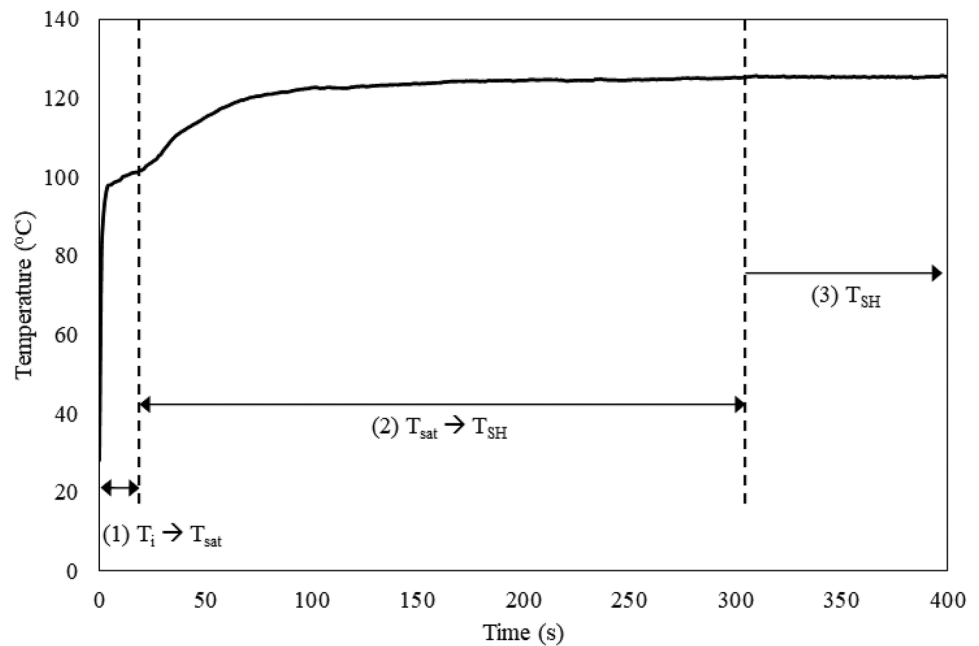
Results and Discussion

Heat Transfer Characteristics of Different Flour Coated Surfaces

Figure 1 shows a representative temperature curve of the flour film on a stainless-steel coupon during superheated steam treatment. The temperature histories of the flour film can show the following three distinct phases:

- (1) The temperature of flour film rapidly increases from the initial temperature to the saturation temperature of steam (100 °C). Larger amount of latent heat energy of superheated steam help to facilitate this temperature increase.
- (2) After reaching the saturation temperature, the temperature gradually increases to the target superheated steam temperature.
- (3) Once the temperature of the flour film reaches the target superheated steam temperature, there is no additional change in temperature during treatment.

Fig. 1 Representative temperature curve of flour film during superheated steam treatment. T_i is initial temperature, T_{sat} is saturation temperature, and T_{SH} is superheated steam temperature



At each superheated steam temperature (250 °C, 210 °C, 170 °C, 150 °C, and 125 °C), preliminary experiments verified the thermal uniformity within the treatment chamber (Table 1). The temperature profiles of flour film on different surfaces at different superheated steam temperature are shown in Fig. 2. We noticed the thermal degradation of rubber with exposure to superheated steam temperature above 125 °C (similar observations were reported by Das et al., 2007). Thus, the samples on rubber coupons were treated only at 125 °C.

Regardless of superheated steam temperature and coupon surface, the temperature of the flour rapidly increased to 100 °C because of the high amount of latent heat released by condensation of steam ($t_{cond} < 11.1$ s) (Table 1). As the superheated steam temperature increased from 125 to 250 °C, t_{cond} decreased because the high temperature of superheated steam hastened the heat transfer at the surface of the

flour. The time constant (τ) values for stainless steel were larger than that for concrete and rubber at each superheated steam temperature, which means that the heating rates on stainless steel were lower than that on concrete and rubber.

The come-up time to reach various target temperature was significantly ($p < 0.05$) longer on stainless steel than that on concrete and rubber (Fig. 3). This is possibly due to the higher thermal diffusivity of stainless steel ($3.54 \times 10^{-6} \text{ m}^2/\text{s}$ – $3.92 \times 10^{-6} \text{ m}^2/\text{s}$) compared to those of concrete ($0.54 \times 10^{-6} \text{ m}^2/\text{s}$ – $0.68 \times 10^{-6} \text{ m}^2/\text{s}$), and rubber ($0.14 \times 10^{-6} \text{ m}^2/\text{s}$) in the ranges of temperature from 125 to 250 °C (Kim, 1975; Pinedo et al., 2018; Zehfuß et al., 2020). Because of the high thermal diffusivity of stainless steel, it acted as a heat sink and dissipated the heat to the environment while concrete and rubber surfaces relatively acted as a thermal insulator so that the temperature of flour rapidly increased.

Table 1 Condensation time and time constant values for flour film on different coupons during superheated steam treatment

Temperature (°C)	Coupon	Condensation time (s)	Time constant (s)
250.5 ± 0.4	Stainless steel	2.0 ± 0.7	39.8
	Concrete	1.8 ± 0.4	14.1
210.6 ± 0.3	Stainless steel	2.6 ± 0.5	66.5
	Concrete	2.1 ± 0.3	21.4
170.6 ± 0.3	Stainless steel	4.7 ± 0.9	93.1
	Concrete	2.7 ± 0.7	34.0
150.5 ± 0.3	Stainless steel	8.8 ± 1.4	173.6
	Concrete	3.1 ± 0.7	89.0
	Stainless steel	11.1 ± 1.1	42.7
125.4 ± 0.3	Concrete	3.4 ± 1.6	30.6
	Rubber	3.1 ± 0.9	29.5

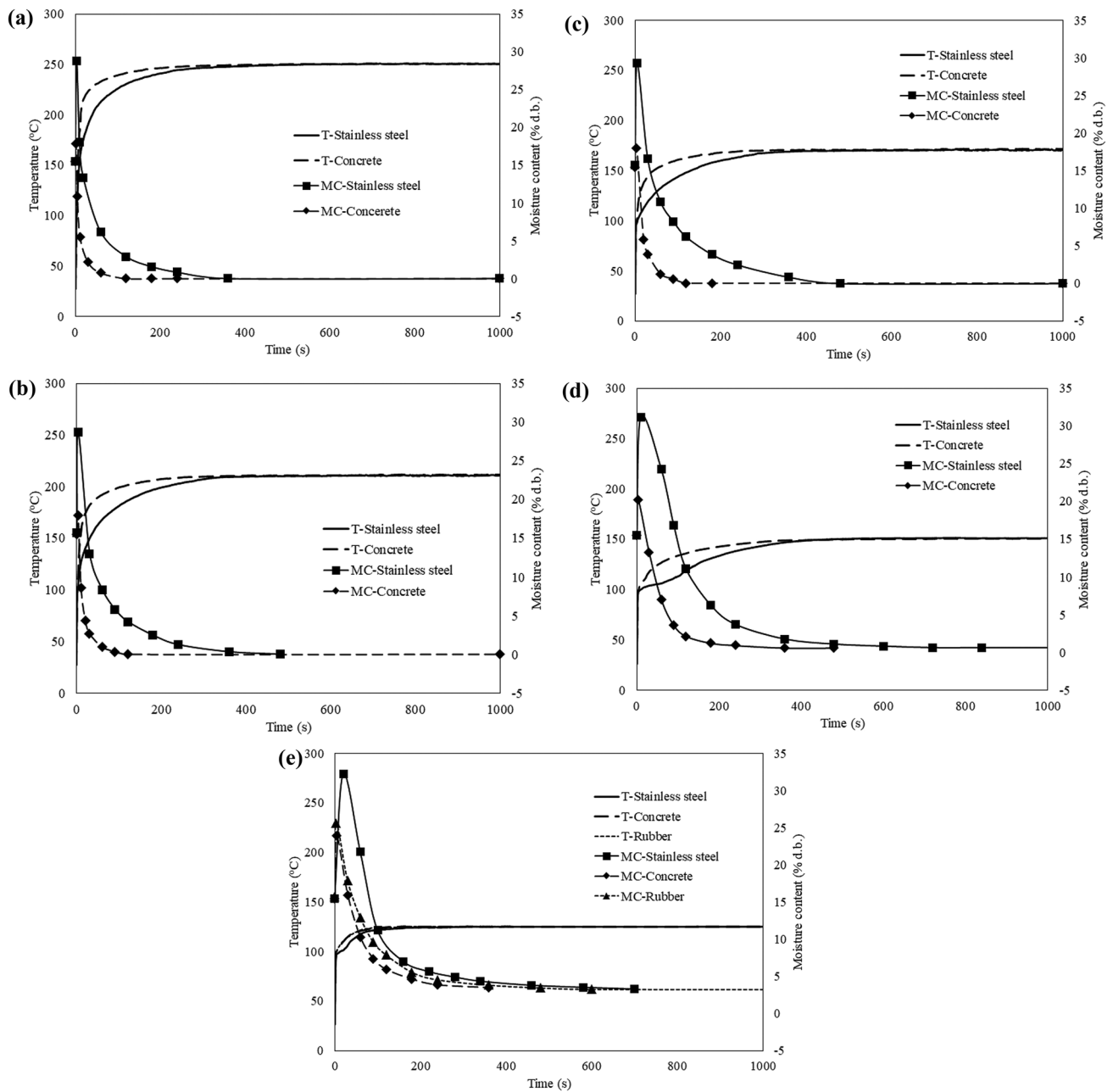


Fig. 2 Changes in the temperature (T) and moisture content (MC) of flour film on different surfaces during superheated steam treatment at (a) 250 °C, (b) 210 °C, (c) 170 °C, (d) 150 °C, and (e) 125 °C

Moisture Transfer Characteristics of Flour on Different Surfaces

Equilibrium moisture content (M_{eq}) of flour determined at different superheated steam temperatures is shown in Fig. S1. Even though the temperature of superheated steam is higher than boiling point of water, the M_{eq} of flour film was higher than 0% in the range of temperature from 125 to 160 °C. Since the partial vapor pressure of superheated steam (vapor) is essentially the same as the atmospheric

pressure, it requires temperatures higher than its boiling point to remove the bound water in drying materials (Tang & Cenkowski, 2001). In this study, the M_{eq} of flour decreased as the superheated steam temperature increased, and it reached 0% at 165 °C.

Similar to the heat transfer characteristics of superheated steam, the change in moisture content of the flour film during superheated steam treatment consisted of 3 distinct stages (Fig. 4):

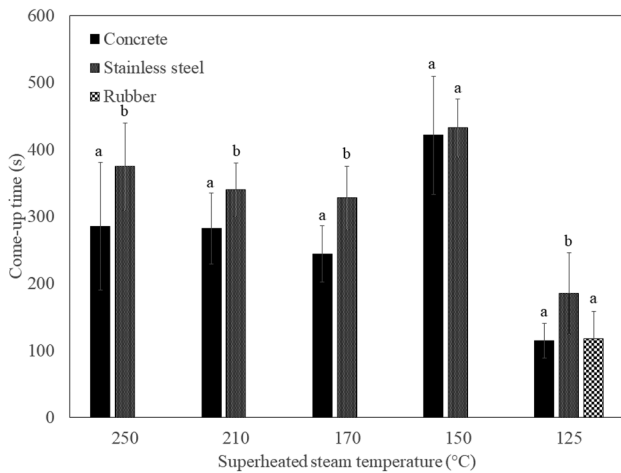
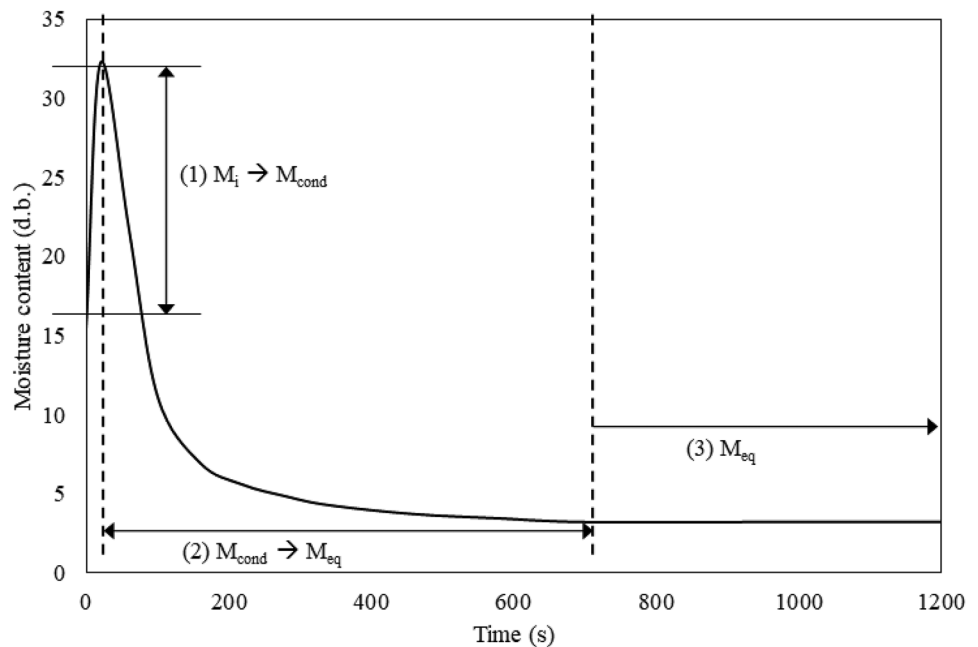


Fig. 3 Temperature come-up time on different surfaces at different superheated steam temperatures. Bars with different letters are significantly different ($p < 0.05$) at each superheated steam temperature

- (1) Flour film absorbed moisture due to the initial condensation of steam until the surface temperature of flour film reaches the saturation temperature of steam. The quantity of condensed moisture may depend upon various factors such as thermal diffusivity of material being heated, its initial moisture content, and degree of superheat of the steam (Beeby & Potter, 1985; Karimi, 2010).
- (2) As the temperature of flour film increases above the saturation temperature, the moisture content of flour film after initial condensation starts to decrease to M_{eq} .

Fig. 4 Representative moisture content curve of flour film during superheated steam treatment. M_i is initial moisture content, M_{cond} is moisture content after initial condensation, and M_{eq} is equilibrium moisture content



- (3) There is no further dehydration once it reaches M_{eq} . The changes in moisture content of flour on different surfaces during superheated steam treatment are shown in Fig. 2.

As previously stated, t_{cond} increased as the superheated steam temperature decreased (Table 1). Similarly, M_{cond} also increased with decreasing superheated steam temperature (Table 2). The D values also increased as the superheated steam temperature increased because increasing temperature hastens the mass transfer of drying materials (Park et al., 2018). The highest D values were observed on concrete at each superheated steam temperature (Table 2). Concrete is a porous material that vapor can diffuse through, in contrast to non-porous materials such as stainless steel and rubber (Zhang et al., 2011). Thus, the flour on concrete dehydrated faster than that on stainless steel and rubber. The results showed that there is dynamic heat and mass (moisture) transfer between treated surfaces and superheated steam. This differentiates itself from treating the surface with hot air.

The Inactivation of *Geobacillus stearothermophilus* Spores in Flour on Different Surfaces

Figure 5 reports the inactivation for *G. stearothermophilus* spores in flour during superheated steam treatment. The temperature of superheated steam significantly affected the inactivation of *G. stearothermophilus* spores on both concrete and stainless steel ($p < 0.05$). At 125 °C and 150 °C, 5 log reductions were not achieved even after treating the surface

Table 2 Parameters describing the moisture transfer characteristics for flour film on different coupons during superheated steam treatment

Temperature (°C)	Coupon	Moisture content after initial condensation (% d.b.)	Moisture diffusivity (10^{-4} mm. ² /s)
250.5 ± 0.4	Stainless steel	28.8 ± 0.5	1.27
	Concrete	17.8 ± 0.3	4.66
210.6 ± 0.3	Stainless steel	28.7 ± 0.5	1.07
	Concrete	18.0 ± 0.2	3.81
170.6 ± 0.3	Stainless steel	29.3 ± 0.4	0.85
	Concrete	18.0 ± 0.2	3.50
150.5 ± 0.3	Stainless steel	31.2 ± 0.4	0.80
	Concrete	20.2 ± 0.2	1.66
125.4 ± 0.3	Stainless steel	32.2 ± 0.3	0.76
	Concrete	23.9 ± 0.2	1.17
	Rubber	25.6 ± 0.1	0.92

for a total treatment time of 1800s. The total treatment times required for 5 log reductions at 170 °C were 1200 s on both concrete and stainless-steel coupons. As the superheated steam temperature increased from 170 to 250 °C, the total time required for 5-log reduction decreased to 180 s and 240 s on stainless steel and concrete, respectively. This treatment time occurred before the temperature come-up time (374 s and 285 s for stainless steel and concrete, respectively) for the treatment at 250 °C. This result clearly shows that the total treatment time can be reduced by increasing superheated steam temperature. The dependence of microbial inactivation rate on superheated steam temperature observed in this study agreed with those reported by Cenkowski et al. (2007) and Park et al. (2021).

The multi-way ANOVA test showed that various treatment variables (superheated steam temperature, treatment time, and type of coupon) significantly affected the inactivation of *G. stearo-thermophilus* spores ($p < 0.05$). It should be noted here that the inactivation of *G. stearo-thermophilus* spores was greater on stainless steel than that on concrete and rubber even though the temperature of flour was lower on stainless steel until it reached each target temperature. This is possibly due to higher moisture content of flour on stainless steel than that on concrete and rubber, which reduces the thermal resistance of *G. stearo-thermophilus* spores (Cunningham et al., 2007). Similar trends in the effect of moisture content or water activity on the thermal inactivation of microorganisms during superheated steam treatment were reported by Hu et al. (2016) and Park et al. (2021). The thermal resistance of *Enterococcus faecium* in peanut butter decreased log-linearly with increasing water activity during superheated steam treatment (Park et al., 2021). In the study of Hu et al. (2016), soaked wheat kernels with a moisture content of 16.0% (w.b.) showed higher inactivation of total bacteria and *Bacillus* spp. compared to those in raw wheat kernels with a moisture content of 12.1% (w.b.).

Our result indicated that the inactivation of *G. stearo-thermophilus* spores was greatly affected by the dynamic heat and moisture transfer between superheated steam and different surfaces.

Modeling the Inactivation of *Geobacillus stearo-thermophilus* Spores in Flour on Different Surfaces

To describe the inactivation kinetics of *G. stearo-thermophilus* spores, 3 inactivation models (Eqs. (7), (9), and (11)) were used to fit the inactivation data at 125 °C, 170 °C, and 250 °C (Table 3).

Model B was able to fit the inactivation curves of *G. stearo-thermophilus* spore. However, z_{RH} in model B was determined to be -45.6%, which means the D value of *G. stearo-thermophilus* increase as the RH of superheated steam increased. Since increasing relative humidity is generally known to accelerate microbial inactivation (Casulli et al., 2018; Yang et al., 2021), the model B prediction may be unrealistic. Model B possibly overfitted the experimental data.

In model C, D_{ref} , T_{iv} , and z_M were determined to be 243.7 s, 165.6 °C, and 16.6%, respectively (Table 3). Log D values of *G. stearo-thermophilus* spore determined from model C are shown in Fig. S2. It is evident that D values decrease with increase in temperature beyond T_{iv} but at a reduced rate. Thus, two different temperature sensitivity (z_T) values were estimated. When $T < T_{iv}$, z_T was determined to be 37.8 °C. For $T > T_{iv}$, z_T was 122.2 °C.

Researchers reported a z_T value of 9.6 to 15.6 °C during conventional heat treatment of *G. stearo-thermophilus* spore (Cunningham et al., 2007; López et al., 1996). For dry heat, the *G. stearo-thermophilus* spore (ATCC 7953) reported to have a z_T value of 56.8 °C in the temperature range from 150 to 200 °C (Wood et al., 2010). The z_T value (37.8 °C) in this

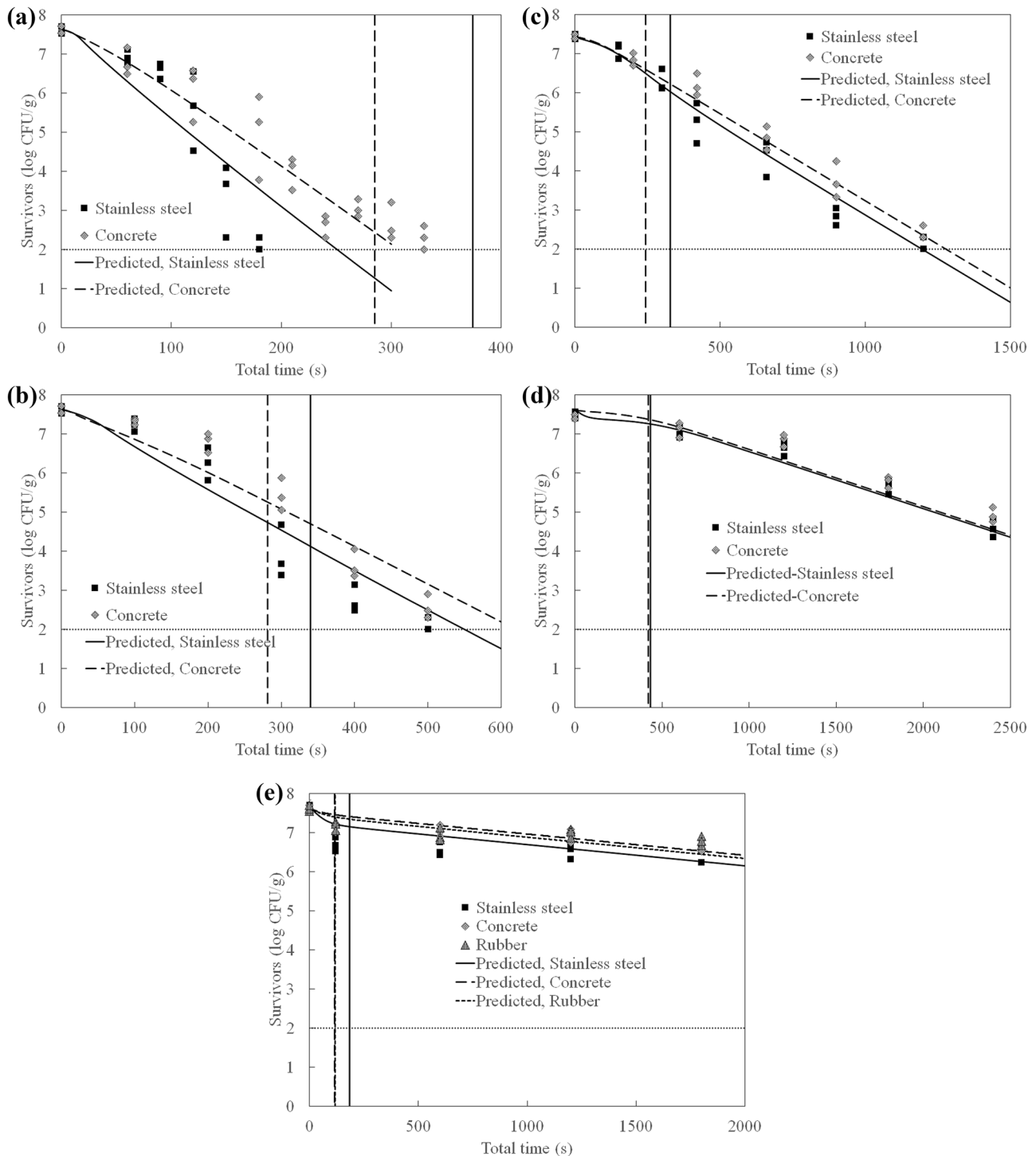


Fig. 5 Inactivation of *Geobacillus stearothermophilus* spore in flour on different coupon surfaces at (a) 250 °C, (b) 210 °C, (c) 170 °C, (d) 150 °C, and (e) 125 °C. Predicted is the estimated spore inactivation by model C, and come-up time is the temperature come-up time for each coupon

study ($T < T_{iv}$) was in between the z_T values reported for wet heat and dry heat conditions. For $T > T_{iv}$, z_T value (122.2 °C) was higher. In this study, certain strain of *G. stearothermophilus* (ATCC 7953) was used as a biological indicator. Strain to strain variations could also influence temperature sensitivity values.

Model Validation

The inactivation models were validated using independent inactivation data at 150 °C and 210 °C (Table 3). The largest RMSE value was observed in model B even though model B has more parameters than model A, indicating that

Table 3 Estimated parameters and validation of the inactivation models

Model	Parameter	Reference value	Estimate	95% lower CI	95% upper CI	Relative error (%)
A	D_{ref} (s)		377.1	308.5	445.8	9.3
	z_T (°C)		83.0	75.9	90.2	4.4
	z_M (%)		29.4	14.2	44.6	26.4
	T_{ref} (°C)	165.6				
	M_{ref} (%)	0.0				
	$RMSE$ (log CFU/g)		1.03			
	B_f			1.47		
B	D_{ref} (s)		276.6	249.2	303.9	5.1
	z_T (°C)		168.0	134.7	201.3	10.1
	z_M (%)		28.0	21.9	34.0	11.1
	z_{RH} (%)		-45.6	-54.7	-36.6	10.2
	T_{ref} (°C)	165.6				
	M_{ref} (%)	0.0				
	$RMSE$ (log CFU/g)		1.38			
	B_f		11.89			
C	D_{ref} (s)		243.7	222.6	264.7	4.4
	T_{iv} (°C)		165.6	147.6	183.7	5.5
	z_{T1} (T < T_{iv}) (°C)		37.8	33.9	41.8	5.3
	z_{T2} (T ≥ T_{iv}) (°C)		122.2	109.4	134.9	5.3
	z_M (%)		16.6	14.4	18.9	6.8
	T_{ref} (°C)	165.6				
	M_{ref} (%)	0.0				
	$RMSE$ (log CFU/g)		0.53			
	B_f		1.22			

B_f bias factor, CI confidence interval, D_{ref} D value at a reference condition, M_{ref} reference moisture content, $RMSE$ root mean squared error, T temperature, T_{iv} inversion temperature, T_{ref} reference temperature, z_T temperature sensitivity, z_M moisture content sensitivity, z_{RH} relative humidity sensitivity

model B overfitted the data and cannot reliably predict the inactivation of *G. stearothermophilus* spores, especially at temperatures lower than T_{iv} where the RH of superheated steam is relatively high (Table 3). Compared to models A and B, model C reasonably predicted the inactivation of *G. stearothermophilus* spores with an overall $RMSE$ of 0.53 (Figs. 5 and S3). This illustrates that inactivation of *G. stearothermophilus* spores on different surfaces can be reasonably predicted equation a mathematical model (Eq. (11)) that consider the temperature and moisture content profiles along with inversion temperature. As empirical model, the model should be used within the range of experimental conditions it was developed. Extrapolation of the model beyond the range of experimental conditions may produce erroneous results.

Role of Inversion Temperature in Spore Inactivation

The relevance of inversion temperature of superheated steam in microbial inactivation was reported by Park et al. (2021). In that study, the D values of *E. faecium* in peanut butter greatly decreased as the superheated steam increased

from 125 to 175 °C, but above 175 °C, the inactivation of *E. faecium* was less sensitive to temperature change. These findings were similar with our current finding showing that the inactivation of *G. stearothermophilus* is less sensitive to temperature change (z_T of 122.2 °C) when temperature is higher than T_{iv} (165.6 °C), compared to the inactivation of *G. stearothermophilus* (z_T of 37.8 °C) for temperature below T_{iv} . This T_{iv} value was also corroborated by the change in the M_{eq} of flour at different superheated steam temperatures. M_{eq} of flour decreased as the superheated steam temperature increased and became ≈ 0% at the temperature near T_{iv} (165 °C). This implies that superheated steam behaves as dry heat at $T > T_{iv}$ for the flour sample (Fig S1). Inactivation of *G. stearothermophilus* spores is sensitive to temperature change when the superheated steam temperature is below T_{iv} , while the sensitivity diminishes above T_{iv} where the superheated steam is a completely dry heat.

Superheated steam technology provides a potential opportunity for cleaning and sanitation of food contact surfaces from the dry food processing environment without the use of any chemical detergent. However, further exploration of pilot scale and commercial application is required. The

present study was conducted using a 1-kW lab scale unit. Thus, findings from this study need to be re-validated under industrially relevant conditions using pilot scale equipment. It is worth noting that this technology has been implemented as a surface sanitation technology in hospitals, nursing homes, health care centers, and similar environments (Acar et al., 2020; Annon, 2017; Oztoprak et al., 2019; Van Doornmalen & Kopinga, 2008), but it has not yet been introduced in dry food processing plant environments.

Very limited scholarly articles have evaluated the energy use of superheated steam for dry sanitation applications. Li et al. (2016) compared the energy use of superheated steam and convective dryer. The authors have found that superheated steam has a much lower specific energy consumption (lower than 0.06 kWh/kg water removed) compared to convective drying (between 0.9 and 1.8 kWh/kg water removed).

Conclusions

This study demonstrated that the inactivation of *G. stearo-thermophilus* spores during superheated steam treatment was greatly influenced by the dynamic heat and moisture transfer exchange between superheated steam and different surface materials. Among the materials investigated, possibly due to its higher thermal diffusivity, the stainless-steel surface showed a slower heating rate and longer condensation time than concrete and rubber. The inactivation of *G. stearo-thermophilus* spores was greater on stainless steel than on concrete or rubber ($p < 0.05$) because of the higher moisture content of flour on stainless steel, which might have reduced the thermal resistance of *G. stearo-thermophilus* spores. A mathematical model that considered the inversion temperature of superheated steam, the surface temperature and moisture content of flour was found to adequately describe spore inactivation in different surfaces during superheated steam treatment. The knowledge gained from the study can help sanitation experts in evaluating application of superheated steam in dry sanitation of different food plant surfaces.

Supplementary Information The online version contains supplementary material available at <https://doi.org/10.1007/s11947-022-02830-3>.

Acknowledgements Research was conducted at The Ohio State University Food Safety Engineering Laboratory, Center for Clean Food Process Technology Development (u.osu.edu/foodsafetyeng/) in collaboration with Dr. Snyder laboratory, Cornell University. Authors thank Molly Davis, The Ohio State University, for her assistance with proofreading the manuscript. References to commercial products or trade names are made with the understanding that no endorsement or discrimination by The Ohio State University and Cornell University is implied.

Author Contribution Hyeon Woo Park: Conceptualization, data curation, formal analysis, methodology, and writing—original draft. V. M. Balasubramaniam: Conceptualization, data curation, formal analysis, funding acquisition, methodology, project administration, resources, supervision, and writing—review and editing. Abigail B. Snyder: Conceptualization, data curation, formal analysis, funding acquisition, methodology, resources, supervision, and writing—review and editing. J. A. Sekhar: Resources and writing—review and editing.

Funding The authors gratefully acknowledge the financial support for the study from the USDA National Institute of Food and Agriculture, AFRI project 2019–68015-29232 (Transforming sanitation strategies in dry food manufacturing environments).

Data Availability All data generated or analyzed during this study are included in this published article and its supplementary information files.

Declarations

Competing Interest The authors declare no competing interests.

References

- Acar, C., Dincer, I., & Mujumdar, A. (2020). A comprehensive review of recent advances in renewable-based drying technologies for a sustainable future. *Drying Technology*, 1–27.
- Annon. (2017). The truth about steam cleaning. *European Cleaning Journal*. <http://www.europecleaningjournal.com/magazine/articles/special-features/the-truth-about-steam-cleaning>. Access Date May 10 2022
- AOAC. (1990). *Official methods of analysis* (15th ed.). The Association of Official Analytical Chemists.
- Ban, G. H., Yoon, H., & Kang, D. H. (2014). A comparison of saturated steam and superheated steam for inactivation of *Escherichia coli* O157: H7, *Salmonella* Typhimurium, and *Listeria monocytogenes* biofilms on polyvinyl chloride and stainless steel. *Food Control*, 40, 344–350.
- Baranyi, J., Pin, C., & Ross, T. (1999). Validating and comparing predictive models. *International Journal of Food Microbiology*, 48(3), 159–166.
- Beeby, C., & Potter, O. E. (1985). *Steam drying*. Proc. 4th Int. Drying Symp., May 5–8, Kyoto, Japan.
- Bergman, T. L., Incropera, F. P., Lavine, A. S., & DeWitt, D. P. (2011). *Introduction to heat transfer*. John Wiley & Sons.
- Beuchat, L. R., Komitopoulou, E., Beckers, H., Betts, R. P., Bourdichon, F., Fanning, S., Joosten, H. M., & Ter Kuile, B. H. (2013). Low-water activity foods: Increased concern as vehicles of foodborne pathogens. *Journal of Food Protection*, 76(1), 150–172.
- Björk, H., & Rasmuson, A. (1995). Moisture equilibrium of wood and bark chips in superheated steam. *Fuel*, 74(12), 1887–1890.
- Burnett, S. L., & Hagberg, R. (2014). Dry cleaning, wet cleaning, and alternatives to processing plant hygiene and sanitation. In J. B. Gurtler, M. P. Michael, & J. L. Kornacki (Eds.), *The Microbiological Safety of Low Water Activity Foods and Spices* (pp. 85–96). Springer.
- Cai, S., Phinney, D. M., Heldman, D. R., & Snyder, A. B. (2020). All treatment parameters affect environmental surface sanitation efficacy, but their relative importance depends on the microbial target. *Applied and Environmental Microbiology*, 87(1), e01748–e1820.
- Carlsaw, H. S., & Jaeger, J. C. (1959). *Conduction of heat in solids*. Clarendon Press.

- Casulli, K. E., Dolan, K. D., & Marks, B. P. (2021). Modeling the effects of product temperature, product moisture, and process humidity on thermal inactivation of *Salmonella* in pistachios during hot-air heating. *Journal of Food Protection*, 84(1), 47–57.
- Casulli, K. E., Garces-Vega, F. J., Dolan, K. D., Ryser, E. T., Harris, L. J., & Marks, B. P. (2018). Impact of process temperature, humidity, and initial product moisture on thermal inactivation of *Salmonella* Enteritidis PT 30 on pistachios during hot-air heating. *Journal of Food Protection*, 81(8), 1351–1356.
- Cenkowski, S., Pronyk, C., Zmidzinska, D., & Muir, W. E. (2007). Decontamination of food products with superheated steam. *Journal of Food Engineering*, 83(1), 68–75.
- Cunningham, S. E., Magee, T. R. A., Mcminn, W. A. M., Gaze, J. E., & Richardson, P. S. (2007). Thermal resistance of *Bacillus steothermophilus* spores in dried pasta at different stages of rehydration. *Journal of Food Processing and Preservation*, 31(4), 420–432.
- Das, A., Jurk, R., Stöckelhuber, K. W., & Heinrich, G. (2007). Rubber curing chemistry governing the orientation of layered silicate. *Express Polymer Letters*, 1, 717–723.
- Hamawand, I., Yusaf, T., & Bennett, J. (2014). Study and modelling drying of banana slices under superheated steam. *Asia-Pacific Journal of Chemical Engineering*, 9(4), 591–603.
- Hu, Y., Nie, W., Hu, X., & Li, Z. (2016). Microbial decontamination of wheat grain with superheated steam. *Food Control*, 62, 264–269.
- Jo, Y., Bae, H., Kim, S. S., Ban, C., Kim, S. O., & Choi, Y. J. (2019). Inactivation of *Bacillus cereus* ATCC 14579 spore on garlic with combination treatments of germinant compounds and superheated steam. *Journal of Food Protection*, 82(4), 691–695.
- Karimi, F. (2010). Applications of superheated steam for the drying of food products. *International Agrophysics*, 24, 195–204.
- Kim, C. S. (1975). *Thermophysical properties of stainless steels*. Argonne National Laboratory.
- Kim, W. J., Kim, S. H., & Kang, D. H. (2020). Thermal and non-thermal treatment effects on *Staphylococcus aureus* biofilms formed at different temperatures and maturation periods. *Food Research International*, 137, 109432.
- Kondjoyan, A., & Portanguen, S. (2008). Effect of superheated steam on the inactivation of *Listeria innocua* surface-inoculated onto chicken skin. *Journal of Food Engineering*, 87(2), 162–171.
- López, M., González, I., Condón, S., & Bernardo, A. (1996). Effect of pH heating medium on the thermal resistance of *Bacillus steothermophilus* spores. *International Journal of Food Microbiology*, 28(3), 405–410.
- Li, J., Liang, Q. C., & Bennamoun, L. (2016). Superheated steam drying: Design aspects, energetic performances, and mathematical modeling. *Renewable and Sustainable Energy Reviews*, 60, 1562–1583.
- Marinos-Kouris, D., & Maroulis, Z. B. (2020). Transport properties in the drying of solids. In A. S. Mujumdar (Ed.), *Handbook of Industrial Drying* (2nd ed., pp. 113–159). CRC Press.
- Marriott, N. G., Schilling, M. W., & Gravani, R. B. (2016). *Principles of food sanitation* (6th ed.). Springer.
- Moerman, F., & Mager, K. (2016). Cleaning and disinfection in dry food processing facilities. *Handbook of hygiene control in the food industry* (pp. 521–554). Woodhead Publishing.
- Overhults, D. G., White, G. M., Hamilton, H. E., & Ross, I. J. (1973). Drying soybeans with heated air. *Transactions of the ASAE*, 16(1), 112.
- Oztoprak, N., Kizilates, F., & Percin, D. (2019). Comparison of steam technology and a two-step cleaning (water/detergent) and disinfecting (1,000 resp. 5,000 ppm hypochlorite) method using microfiber cloth for environmental control of multidrug-resistant organisms in an intensive care unit. *GMS Hygiene and Infection Control*, 14, Doc15. <https://doi.org/10.3205/dgkh000330>
- Park, H. W., Han, W. Y., & Yoon, W. B. (2018). Drying characteristics of soybean (*Glycine max*) using continuous drying and intermittent drying. *International Journal of Food Engineering*, 14(9–10).
- Park, H. W., Xu, J., Balasubramaniam, V. M., & Snyder, A. B. (2021). The effect of water activity and temperature on the inactivation of *Enterococcus faecium* in peanut butter during superheated steam sanitation treatment. *Food Control*, 125, 107942.
- Pinedo, B., Hadfield, M., Tzanakis, I., Conte, M., & Anand, M. (2018). Thermal analysis and tribological investigation on TPU and NBR elastomers applied to sealing applications. *Tribology International*, 127, 24–36.
- Prachayawarakorn, S., Soponronnarit, S., Wetchacama, S., & Jaisut, D. (2002). Desorption isotherms and drying characteristics of shrimp in superheated steam and hot air. *Drying Technology*, 20(3), 669–684.
- Pronyk, C., Cenkowski, S., & Muir, W. E. (2004). Drying foodstuffs with superheated steam. *Drying Technology*, 22(5), 899–916.
- Ramachandran, R. P., Bourassa, J., Paliwal, J., & Cenkowski, S. (2017). Effect of temperature and velocity of superheated steam on initial condensation of distillers' spent grain pellets during drying. *Drying Technology*, 35(2), 182–192.
- Schwartz, J. P., & Brocker, S. (2002). A theoretical explanation for the inversion temperature. *Chemical Engineering Journal*, 86, 61–67.
- Swasdisevi, T., Devahastin, S., Thanasookprasert, S., & Soponronnarit, S. (2013). Comparative evaluation of hot-air and superheated-steam impinging stream drying as novel alternatives for paddy drying. *Drying Technology*, 31(6), 717–725.
- Tang, Z., & Cenkowski, S. (2000). Dehydration dynamics of potatoes in superheated steam and hot air. *Canadian Agricultural Engineering*, 42(1), 43–49.
- Tang, Z., & Cenkowski, S. (2001). Equilibrium moisture content of spent grains in superheated steam under atmospheric pressure. *Transactions of the ASAE*, 44(5), 1261.
- Van Deventer, H. C., & Heijmans, R. M. H. (2001). Drying with superheated steam. *Drying Technology*, 19(8), 2033–2045.
- Van Doornmalen, J., & Kopinga, K. (2008). Review of surface steam sterilization for validation purposes. *American Journal of Infection Control*, 36(2), 86–92.
- Volchkov, E. P., Leontiev, A. I., & Makarova, S. N. (2007). Finding the inversion temperature for water evaporation into an air-steam mixture. *International Journal of Heat and Mass Transfer*, 50(11–12), 2101–2106.
- Wang, Y., Wu, A., Zhang, L., Jin, F., & Liu, X. (2018). Investigating the effect of solid components on yield stress for cemented paste backfill via uniform design. *Advances in Materials Science and Engineering*, 2018, 3839174.
- Wood, J. P., Lemieux, P., Betancourt, D., Kariher, P., & Gatchalian, N. G. (2010). Dry thermal resistance of *Bacillus anthracis* (Sterne) spores and spores of other *Bacillus* species: Implications for biological agent destruction via waste incineration. *Journal of Applied Microbiology*, 109(1), 99–106.
- Yang, R., Xie, Y., Lombardo, S. P., & Tang, J. (2021). Oil protects bacteria from humid heat in thermal processing. *Food Control*, 123, 107690.
- Zehfuß, J., Robert, F., Spille, J., & Razafinjato, R. N. (2020). Evaluation of Eurocode 2 approaches for thermal conductivity of concrete in case of fire. *Civil Engineering Design*, 2(3), 58–71.
- Zhang, J., Hou, D., Gao, Y., & Wei, S. (2011). Determination of moisture diffusion coefficient of concrete at early age from interior humidity measurements. *Drying Technology*, 29(6), 689–696.